

THE NIJMEGEN FEL, A FEL OSCILLATOR WITH HIGH SLIPPAGE

P.J.M. van der Slot*, E. van Geijn, K.J. Boller

Mesa⁺, Department of Applied Technology, University of Twente, Enschede, NL
 J. Jalink, W.J. van der Zande, IMM, Radboud University Nijmegen, Nijmegen, NL

Abstract

The Nijmegen Free-Electron Laser (FEL) aims at producing narrow bandwidth radiation for high resolution spectroscopy in the THz regime. To this end, the radio frequency accelerator based FEL will produce a train of phase locked optical pulses. We use the Medusa1D code to simulate the performance of this system at various wavelengths and undulator lengths and estimate the power available in a single line of the phase locked spectrum.

INTRODUCTION

The High Field Magnetic Laboratory at the Radboud University Nijmegen, and other such laboratories worldwide, have made it possible to study molecules in materials in fields with strengths approaching 40 Tesla. All elementary excitation energies increase proportionally. As a consequence strong (> 100 W) and coherent radiation sources are needed from $100 \mu\text{m}$ to 1.5 mm, the so-called THz gap. Narrow bandwidth radiation is best suited for coherent, saturation, and pulse-echo studies. Pulsed intense radiation is best suited for non-linear and time-resolved studies. The parameters of the Nijmegen Free-Electron Laser (NijFEL) have been chosen to provide such a radiation source. An RF accelerator based electron source will provide short electron bunches creating a train of intense micropulses of picosecond duration. A narrow bandwidth, ($\Delta\lambda/\lambda \simeq 10^{-5}$), equals the generation of bandwidth limited pulses (BWL) of hundreds of nanosecond duration. This is achieved by ensuring that the micropulses in the macropulse are fully coherent, either using spontaneous coherence or forcing coherence using an intra-cavity interferometer. It is expected that spontaneous coherence is helped by using electron pulses with lengths comparable to the wavelength to be generated. This implies the design of a FEL oscillator with high slippage.

The zero design parameters to achieve this performance with NijFEL are shown in table 1, and fig. 1 shows the resonant wavelength of NijFEL as a function of the undulator parameter K for different values of the electron beam energy E_b . The ratio of the electron bunch length l_e to the slippage distance $\Delta z_s (= N_u \lambda$ at resonance) varies approximately from 0.015 to 0.3 depending on the actual number of undulator periods and wavelength used. The performance of the NijFEL system is therefore highly dominated by short pulse effects [1]. Because of the long wavelengths (see fig. 1), NijFEL will use a half open resonator

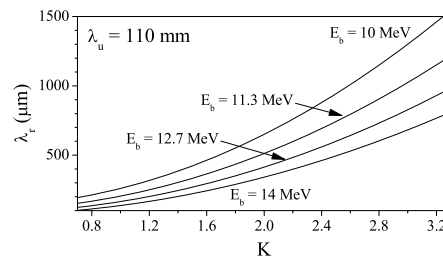


Figure 1: FEL resonant wavelength λ_r as a function of the undulator K parameter for different values of the electron beam energy E_b .

that provides waveguiding between the poles of the undulator.

To determine the performance for various undulator lengths and wavelengths, we use the Medusa1d code. This code retains, in the 1d approximation, all the features of the 3D Medusa code [2, 3]. It includes a simple oscillator model where the radiation output at the undulator's

Table 1: Zero design values for NijFEL. $L_u = N_u \lambda_u$ is the undulator length

Accelerator			
RF frequency	f_{RF}	3	GHz
Bunch charge	Q_b	300	pC
micro pulse duration	t_p	3	ps rms
Beam energy	E_b	10-14	MeV
Emitance (norm.)	ϵ_n	50	mm mrad
Energy spread (rms)	$\Delta\gamma/\gamma$	0.25	%
Duration macropulse	T_m	10-12	μs
Rep. rate macropulses	f_{rep}	≤ 5	Hz
Undulator			
Period	λ_u	110	mm
K (rms)	K	0.7-3.3	
Number of periods	N_u	30-40	
Oscillator & radiation			
Wavelength	λ	0.1-1.5	mm
Final rel. bandwidth	$\Delta\lambda/\lambda$	10^{-5}	
Power (after filtering)	P_u	> 100	W
Total roundtrip loss	α_L	5-20	%
Waveguide height	h	10	mm
Length	L_r	L_u+2	m

* p.j.m.vanderslot@tnw.utwente.nl

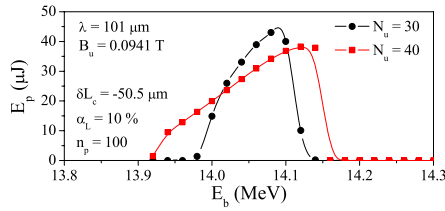


Figure 2: E_p versus E_b after $n_p = 100$ passes for $N_u = 30$ (circles) and 40 (squares).

exit is multiplied by $1 - \alpha_L$, α_L being the total single pass cavity loss, and, after appropriate shifting in the time to compensate for slippage Δz_s and cavity detuning δL_c , is used as input for the next pass. Furthermore, Medusa1d incorporates some 3D effects through Xie's fitting formula [4] which results in an increase of the energy spread of the electrons and a filling factor that includes both diffraction and guiding effects.

1D SIMULATION RESULTS

Medusa1d is not able to model the hybrid resonator that is planned for NijFEL. A geometric filling factor can be used to model overlap between electrons and optical field. However, this does not include possible guiding effects due to the FEL interaction [5, 6]. We therefore compared the filling factor for the hybrid waveguide and the one derived from Ming Xie's fitting formula for an open resonator. The latter is found to be larger than the filling factor for the hybrid waveguide. Apparently, guiding effects in NijFEL are sufficiently strong to influence the filling factor. We therefore consider an open resonator in the remaining part of the paper and use Xie's fitting formula to calculate the filling factor.

Furthermore, an up- and down taper of 2 periods is used at the entrance respectively exit of the undulator to allow proper injection and extraction of the electron beam. Values for parameters are taken from Table 1 unless otherwise specified.

Performance at $\lambda = 100 \mu\text{m}$

In order to produce a narrow bandwidth, the train of coherent optical pulses within the macropulse must be as long as possible. We want to minimize transient effects at the beginning of the macropulse. We therefore evaluate the performance of NijFEL at $\lambda = 100 \mu\text{m}$ for both maximum gain and maximum efficiency settings of the electron beam energy. For an electron beam energy of 14 MeV and a peak undulator field of $B_u = 0.0941 \text{ T}$ we find a maximum single pass, small signal gain for $\lambda = 101 \mu\text{m}$. Figure 2 shows the intracavity optical pulse energy E_p after $n_p = 100$ passes as a function of E_b . The cavity detuning is $\delta L_c = -0.5\lambda$ with respect to a synchronous cavity that is defined by the roundtrip time of an optical pulse in an empty cavity being

FEL projects

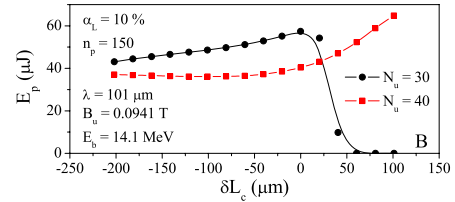
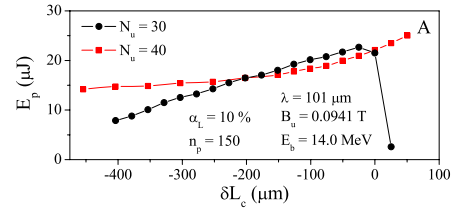


Figure 3: E_p after $n_p = 150$ passes versus δL_c for $N_u = 30$ (circles) and 40 (squares) at maximum single pass, small signal gain (A) and maximum efficiency (B).

a multiple of the time separating two consecutive electron bunches¹. Fig. 2 shows that maximum efficiency is found at slightly higher value for E_b compared to the one required for maximum gain. We therefore have determined the detuning curve for both $E_b = 14 \text{ MeV}$ and 14.1 MeV . The results are shown in fig. 3. Fig. 3A shows that for maximum gain, E_p is about the same for the short and long undulator for $-2\lambda < \delta L_c < 0$ and the longer undulator has a higher pulse energy for smaller cavity lengths. Also the longer undulator shows considerable output energy for $\delta L_c > 0$, where the shorter undulator fails to lase. At maximum efficiency, we find the short undulator having higher optical energies over most of the detuning range investigated, except for cavity lengths larger than the synchronous length where the gain for $N_u = 40$ results in a sharp increase of E_p . We observe that E_p for maximum efficiency setting is about a factor of 2.5 larger than for maximum gain setting.

The number of roundtrips n_b required to reach maximum E_p is shown in fig. 4. This figure shows that indeed for the case of maximum gain significantly fewer roundtrips are required for the optical field to build up to saturation inside the resonator. At this wavelength, a minimum of about 50 roundtrips is required at maximum gain for negative cavity detuning and $N_u = 40$. It increases sharply for positive detuning. The shorter undulator requires at least 50 more roundtrips ($\sim 1.5 \mu\text{s}$) to saturate. Also for maximum efficiency we find that the reduced gain results in a larger value of n_b .

The repetition rate of the optical micropulses will be $f_{rep} = 3 \text{ GHz}$. As a consequence, if all the optical pulses are fully coherent, the resulting frequency spectrum of the train of optical pulses will consist of very narrow lines (linewidth of the order of 10 MHz) separated by the 3 GHz. Filtering of one of the narrow lines does not require a high

¹ $\delta L_c < 0$ means a shorter cavity length

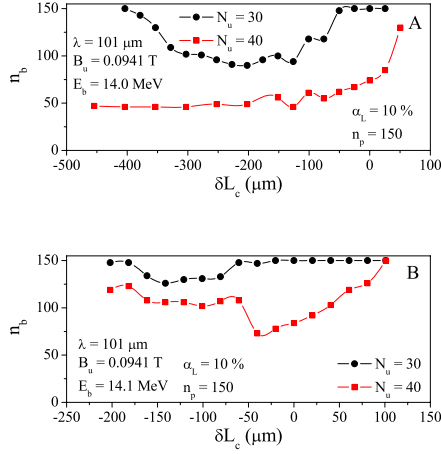


Figure 4: n_b versus δL_c for $N_u = 30$ (circles) and 40 (squares) at maximum single pass, small signal gain (A) and maximum efficiency (B).

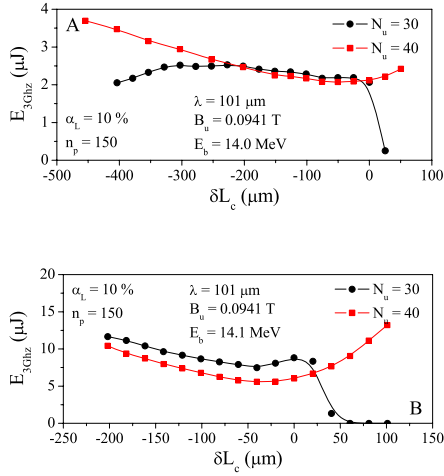


Figure 5: E_{3GHz} versus δL_c for $N_u = 30$ (circles) and 40 (squares) at maximum gain (A) and maximum efficiency (B).

quality etalon as a consequence of the large 3 GHz line spacing. To estimate the energy available after filtering, we have also determined the intracavity optical energy E_{3GHz} of a single optical micropulse in a bandwidth of 3 GHz around the central wavelength. This is an important figure of merit for narrow bandwidth operation of the NijFEL system, as this energy may be concentrated in a line with a width of 10 MHz. This figure of merit is shown in fig. 5 for both the case of maximum gain and maximum efficiency, and again for the two undulator lengths. As expected, we find for $N_u = 40$ that E_{3GHz} increases away from zero detuning [7]. For positive detuning this is due to both a higher pulse energy and an increasingly longer optical pulse. For negative detuning the micropulse energy decreases, how-

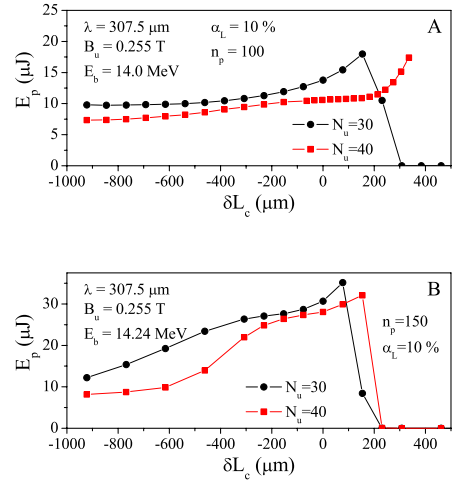


Figure 6: E_p versus δL_c for $N_u = 30$ (circles) and 40 (squares) at maximum gain and 100 passes (A) and maximum efficiency and 150 passes (B).

ever this is more than compensated by the increase in pulse length and hence a narrower spectrum, at least when the detuning is not too large. As a result, the figure of merit increase more rapidly for increasing positive detuning than for decreasing negative detuning. For $N_u = 30$, the behaviour is very similar, albeit that the gain becomes too low for positive detuning values and hence both E_p and E_{3GHz} drop quickly to zero (at least when we limit ourselves to at most 150 roundtrips). Fig. 5A also shows that, for large negative detuning, the figure of merit drops as the increase in pulse duration can not compensate the drop in energy any more.

Performance at $\lambda = 300 \mu\text{m}$

Similar simulations as in the previous section have been done at a wavelength near $\lambda = 300 \mu\text{m}$ as well, using the same beam energy of 14 MeV. Using $B_u = 0.255 \text{ T}$, we find that the maximum single pass, small signal gain is found for $\lambda = 307.5 \mu\text{m}$. Using this wavelength, and varying the beam energy again around the value of 14 MeV, we find, that the maximum efficiency is now near $E_b = 14.24 \text{ MeV}$. Because we expect a higher gain than for $\lambda = 101 \mu\text{m}$, we have taken a maximum of 100 and 150 passes for the high gain respectively maximum efficiency setting. The same results as for $\lambda = 101 \mu\text{m}$ but now for $\lambda = 307.5 \mu\text{m}$ are shown in figs. 6 to 8. Much of the features found for $\lambda = 101 \mu\text{m}$ are also present for the 307.5 μm wavelength. However, for the case of high gain, the figure of merit is higher for the 30 period undulator than for the 40 period one, except for the longest resonator lengths investigated. Also, the higher gain at this wavelength results in an extension of the detuning curve to positive detuning values for the 30 period undulator. For the maximum efficiency setting, and moderate cavity de-

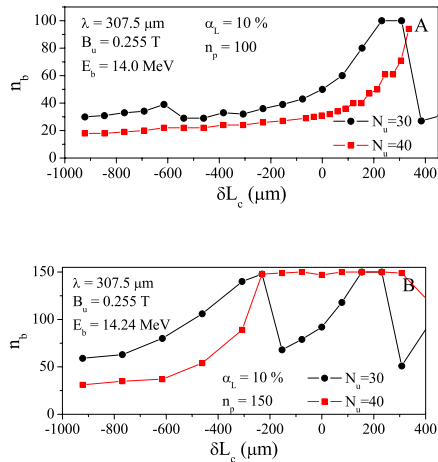


Figure 7: n_b versus δL_c for $N_u = 30$ (circles) and 40 (squares) at maximum gain (A) and maximum efficiency (B).

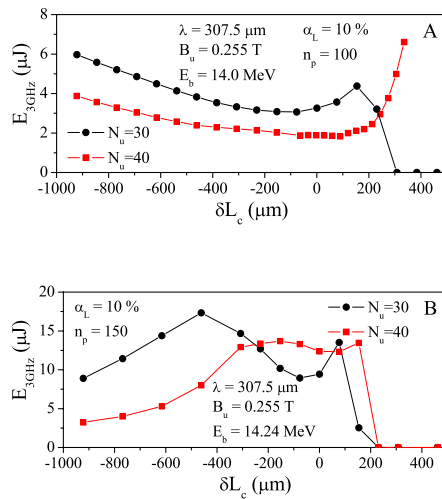


Figure 8: E_{3GHz} versus δL_c for $N_u = 30$ (circles) and 40 (squares) at maximum gain and 100 passes (A) and maximum efficiency and 150 passes (B).

tuning, the 40 period undulator has a slightly higher figure of merit, while for large negative detuning, the 30 period undulator has the higher figure of merit. This may be due to the fact that we used the same E_b for both undulator lengths while the actual value for optimum energy extraction may differ slightly (see fig. 2). Note, that for $N_u = 40$ and $\delta L_c > -300 \mu\text{m}$, E_p is limited by the maximum number of roundtrips used in the simulation. Comparing the two wavelength, we find that for $N_u = 40$ the minimum figure of merit is about the same for both wavelengths at maximum gain setting, while for maximum efficiency and at slightly negative detuning values the figure of merit is a factor of two higher at $307.5 \mu\text{m}$. For the shorter undula-

FEL projects
 tor it is the other way around: at maximum gain, the figure of merit is about a factor of 2 larger for the wavelength $\lambda = 307.5 \mu\text{m}$, and for maximum efficiency it is about the same for the two wavelengths.

DISCUSSION AND CONCLUSION

In the simulation, the NijFEL system can either be set to produce maximum gain or maximum efficiency. For the first setting, the buildup time is smallest and we would expect the smallest bandwidth after filtering provided that the whole train of micropulses is fully coherent. The optical micro pulse energy is however significantly lower than can be obtained for the maximum efficiency settings. As a consequence, the figure of merit is also significantly higher for the maximum efficiency setting. Note that since Medusa1d is set up to use one frequency, it only calculates the optical energy in a finite bandwidth around this frequency. Thus, the resulting bandwidth may be smaller than the gain bandwidth of the laser. Hence, Medusa1d will underestimate the optical energy that can be produced by NijFEL.

The range of values for the figure of merit available through tuning the length of the cavity is the same for both undulator lengths at the longer wavelength, while for $\lambda = 101 \mu\text{m}$ the range is larger for $N_u = 40$.

For the parameters investigated, the minimum figure of merit is $2 \mu\text{J}$. Assuming that half of α_L is due to outcoupling of the radiation, and using the 3 GHz repetition rate of the micropulses, we expect at least 300 W to be available in the strongest spectral line of a fully coherent macropulse. By optimising the detuning, the figure of merit can be at least a factor of 3 to 5 larger, hence, it seems that the design goals for narrow bandwidth operation of NijFEL can be realised with either undulator length. The performance has to be evaluated at other wavelengths as well before the optimum undulator length can be determined.

ACKNOWLEDGEMENT

We would like to thank Lex van der Meer of the FOM Institute for Plasma Physics Rijnhuizen for the useful discussions.

REFERENCES

- [1] W.B. Colson, in "Free-Electron Laser Handbook", eds. W.B. Colson, C. Pellegrini and A. Renieri (Elsevier, Amsterdam, 1990), Chap. 5.
- [2] H.P. Freund, S.G. Biedron, and S.V. Milton. IEEE J. Quantum Electron. **36**, 275 (2000).
- [3] H.P. Freund. Phys. Rev. STAB, **8**, 110701 (2005).
- [4] M. Xie. Nucl. Instrum. Methods Phys. Res., **A445**, 59 (2000).
- [5] E.T. Scharlemann, A.M. Sessler, J.S. Wurtele. Phys. Rev. Lett. **54**, 1925 (1985).
- [6] G.T. Moore. Nucl. Instrum. Methods Phys. Res., **A250**, 381 (1986).
- [7] A.M. Macleod, et.al., Phys. Rev. E **62**, 4215 (2000).